Atmos. Chem. Phys., 13, 7343–7358, 2013
www.atmos-chem-phys.net/13/7343/2013/
doi:10.5194/acp-13-7343-2013

Atmospheric Chemistry and Physics Open Access

CO, NO_x and $^{13}CO_2$ as tracers for fossil fuel CO_2: results from a pilot study in Paris during winter 2010

M. Lopez[1], M. Schmidt[1], M. Delmotte[1], A. Colomb[2,*], V. Gros[1], C. Janssen[3], S. J. Lehman[4], D. Mondelain[3,], O. Perrussel[5], M. Ramonet[1], I. Xueref-Remy[1], and P. Bousquet[1]**

[1]Laboratoire des Sciences du Climat et de l'Environnement (LSCE), Unité mixte CEA-CNRS-UVSQ, UMR8212, 91191 Gif-sur-Yvette, France
[2]Laboratoire Interuniversitaire des Systèmes Atmosphériques (LISA), CNRS-IPSL, 94010 Creteil, France
[3]Laboratoire de Physique Moléculaire pour l'Atmosphère et l'Astrophysique (LPMAA), CNRS, Université Pierre et Marie Curie, 75005 Paris, France
[4]Insitute of Arctic and Alpine Research (INSTAAR), University of Colorado, Boulder, USA
[5]AIRPARIF, Association de Surveillance de la Qualité de l'Air en Ile-de-France, Paris, France
[*]now at: Laboratoire de Métrologie Physique (LaMP), CNRS, 63171 Aubière, France
[**]now at: Laboratoire Interdisciplinaire de Physique (LiPhy), CNRS, Université Joseph Fourier, 38402 Saint Martin d'Hères, France

Correspondence to: M. Lopez (morgan.lopez@lsce.ipsl.fr)

Received: 19 December 2012 – Published in Atmos. Chem. Phys. Discuss.: 22 January 2013
Revised: 20 June 2013 – Accepted: 21 June 2013 – Published: 1 August 2013

Abstract. Measurements of the mole fraction of the CO_2 and its isotopes were performed in Paris during the MEGAPOLI winter campaign (January–February 2010). Radiocarbon ($^{14}CO_2$) measurements were used to identify the relative contributions of 77 % CO_2 from fossil fuel consumption (CO_2ff from liquid and gas combustion) and 23 % from biospheric CO_2 (CO_2 from the use of biofuels and from human and plant respiration: CO_2bio). These percentages correspond to average mole fractions of 26.4 ppm and 8.2 ppm for CO_2ff and CO_2bio, respectively. The $^{13}CO_2$ analysis indicated that gas and liquid fuel contributed 70 % and 30 %, respectively, of the CO_2 emission from fossil fuel use. Continuous measurements of CO and NO_x and the ratios $\frac{CO}{CO_2ff}$ and $\frac{NO_x}{CO_2ff}$ derived from radiocarbon measurements during four days make it possible to estimate the fossil fuel CO_2 contribution over the entire campaign. The ratios $\frac{CO}{CO_2ff}$ and $\frac{NO_x}{CO_2ff}$ are functions of air mass origin and exhibited daily ranges of 7.9 to 14.5 ppb ppm^{-1} and 1.1 to 4.3 ppb ppm^{-1}, respectively. These ratios are consistent with different emission inventories given the uncertainties of the different approaches. By using both tracers to derive the fossil fuel CO_2, we observed similar diurnal cycles with two maxima during rush hour traffic.

1 Introduction

Worldwide, approximately 20 "megacities" have a population of more than 10 million inhabitants. According to the United Nations, half of the world's population now lives in cities, and in the near future, the number of megacities and their population density figures are expected to grow considerably. In the context of global warming and in the framework of the Kyoto Protocol, it is important to better characterise greenhouse gas (GHG) emissions from megacities, which constitute a significant emission source at the global scale. More than 70 % of global fossil fuel CO_2 emissions are concentrated in cities (Duren and Miller, 2012).

With 12 million inhabitants (approximately 18 % of the French population), Paris and its suburbs constitute the largest megacity in Europe. According to the regional French emission inventory provided by AirParif (http://www.airparif.asso.fr/), CO_2 emissions from Paris and its agglomeration (the Ile-de-France region or IdF) were 50 Mt in 2005, or 13 % of the total French anthropogenic CO_2 emissions, although the IdF region, with a surface area of 12 011 km^2, composes only 1.8 % of the French territory. The annual CO_2 emission density within the IdF region increases from

approximately 5000 t CO_2 km^{-2} limits of the suburbs to approximately 70 000 t CO_2 km^{-2} at the centre of Paris, reflecting the change in population density. Based on the Kyoto Protocol, France is committed to reducing its greenhouse gas emissions by 8 % with respect to its 1990 emissions by 2012. A decrease of 6.0 % was observed in 2010 compared to the reference year 1990, primarily due to reductions in N_2O and CO_2 emissions (CITEPA, 2012). In addition, France adopted the "climate and energy package", which aims to reduce greenhouse gas emissions by 20 % with respect to the emissions of 2005 by 2020.

Currently, regional and local GHG emissions data are primarily derived from statistical inventories that are gathered using a bottom-up method that involves the compilation of activity and process data. Economic statistics are gathered from the local to the national level to produce gridded maps of GHG emissions (EDGAR: Olivier et al., 2001; Olivier and Berdowsky, 2001). Peylin et al. (2011) showed that such emission inventories can vary up to 40 % on the national scale even for developed countries like the Netherlands, where we can expect the best datasets available for use in compiling the inventory. Atmospheric measurements can provide an alternative to develop methods of emission verification, in association with bottom-up inventories. Atmospheric methods (top-down methods) rely on a combination of high-precision measurements of atmospheric mole fractions of GHGs such as CO_2 as well as on measurements of atmospheric tracers and atmospheric transport models. At global to regional scales, inverse models have been used successfully to quantify GHG emissions for CO_2 (Rayner and Law, 1999; Bousquet et al., 2000; Rödenbeck et al., 2003; Peylin et al., 2005), CH_4 (Rödenbeck, 2005; Bousquet et al., 2006) and N_2O (Hirsch et al., 2006; Thompson et al., 2011). On the local and regional scales, continuous observations of GHGs can be combined with observations of radon-222, which is used as a tracer for atmospheric dilution (van der Laan et al., 2009; Yver et al., 2009; Hammer and Levin, 2009) to estimate surface emissions.

The use of atmospheric measurements of CO_2 to estimate surface emissions in urban areas is of growing interest. During the last several years, a few projects focusing on quantifying CO_2 fluxes from cities using top-down approaches have emerged in the USA and in France, including the InFLUX project in Indianapolis, USA (http://influx.psu.edu/), the Los Angeles Megacity project (Duren and Miller, 2012) and the CO_2-Megaparis project in Paris (https://co2-megaparis.lsce.ipsl.fr). One challenging issue associated with the atmospheric top-down approach is the attribution of emissions to specific processes. The first step in this process is to distinguish between CO_2 emitted from anthropogenic activities and CO_2 emitted from biospheric activities. Even in urban areas, variations in the atmospheric CO_2 mole fraction contain signatures from both fossil fuel combustion and biogenic sources. These signatures can be decrypted by additional information that is provided by specific tracers. Only $^{14}CO_2$ measurements allow for the direct quantification of the contribution of fossil fuel CO_2 to observed CO_2 mole fractions (Levin et al., 2003; Turnbull et al., 2006; Vogel et al., 2010) because CO_2 from fossil fuels does not contain ^{14}C. Levin and Karstens (2007) showed that fossil fuel emissions and biospheric fluxes are of similar orders of magnitude in Europe. Because precise $^{14}CO_2$ measurements are difficult to perform, carbon monoxide is often used as a tracer for fossil fuel CO_2 emissions (CO_2ff) in order to separate the biospheric and the fossil fuel components from the total measured CO_2 mole fraction. The CO / CO_2ff ratio depends on the condition of combustion and on the fuel type, and can range from 17.5 ppb CO ppm^{-1} CO_2 for industrial sources and 14.5 ppb CO ppm^{-1} CO_2 for residential heating to 5.3 ppb CO ppm^{-1} CO_2 for traffic according to the national emission inventories by the Centre Interprofessionnel Technique d'Etude de la Pollution Atmospherique (CITEPA, http://www.citepa.org/) for the year 2010 in France. From 2000 to 2010, improvements in combustion efficiency due to regulations that are intended to improve air quality led to a significant reduction in CO emissions and also to changes in CO / CO_2ff fossil fuel ratios, which decreased from 20 to 13 ppb CO ppm^{-1} CO_2 in France. This reduction was primarily caused by the introduction of catalytic converters for cars, which decreased the road traffic CO / CO_2ff ratio from 21 to 5 ppb CO ppm^{-1} CO_2.

The European project MEGAPOLI (Megacities: Emissions, urban, regional and Global Atmospheric POLlution and climate effects, and Integrated tools for assessment and mitigation, http://www.megapoli.info) aims to assess the impact of megacities on air pollution, to quantify the feedback regarding megacity air quality and to develop integrated tools for predicting air pollution in megacities. To address these three objectives, the MEGAPOLI project organised two intensive measurement campaigns in Paris: one in July 2009 and one in January–February 2010. During the campaigns, numerous atmospheric pollutants and parameters were monitored by different groups (Royer et al., 2011; Healy et al., 2012; Dolgorouky et al., 2012). The French Atmospheric Network for Greenhouse Gases Monitoring (RAMCES), which is part of the Laboratory for Climate and Environmental Sciences (LSCE), participated in the frame of the CO_2-Megaparis project to the measurement campaign in the winter of 2010, which extended from 15 January to 19 February. During this campaign, we focused on continuous CO_2 and CO measurement in Paris and the Plateau of Saclay (20 km south-west of Paris, Sect. 2). In addition, air was sampled in flasks for $^{14}CO_2$ analysis (Sects. 2.2.2 and 3.1). Radiocarbon and stable CO_2 isotope measurements were used to compute the respective contributions of fossil fuels and biospheric CO_2 to the overall CO_2 mole fraction in Paris (Sects. 3.2 and 3.3). These direct estimations of CO_2ff were used to evaluate the potential of alternative proxies to radiocarbon such as CO and NO_x (Sect. 3.4).

2 Methods

2.1 Description of measurement stations

2.1.1 Paris

Paris is the largest city in France; it has 2.2 million inhabitants (source: INSEE, January 2009) and a population density of 21 196 inhabitants per square kilometre, which is one of the highest densities in Europe. Paris and its suburbs include several industrial and transportation hot spots, although numerous industrial activities were removed from the Paris agglomeration in the 1960s. Two sites were instrumented for atmospheric measurements within the city centre during the MEGAPOLI campaign (see Fig. 1). The Laboratoire de l'Hygiène de la Ville de Paris (LHVP), located at 48°50′ N, 2°21′ E and at 62 m above sea level (a.s.l.), lies within the southern part of Paris (13th district). This laboratory is located on the edge of the Parc de Choisy, approximately 100 m from a main road. A large number of instruments were deployed at the LHVP station to monitor atmospheric compounds such as aerosols, volatile organic compounds (VOCs), ozone, nitrogen oxides ($NO_x = NO + NO_2$) and meteorological parameters. A cavity ring-down spectrometer (CRDS) was installed for continuous atmospheric carbon dioxide (CO_2) and carbon monoxide (CO) measurement, and a flask sampling unit was also installed. All inlet lines were positioned on the roof of the LHVP, 15 m above the ground level (a.g.l.).

A second site was equipped for atmospheric measurements at the QualAir station in Jussieu (http://qualair.aero.jussieu.fr/), a campus of University Pierre et Marie Curie, 48°51′ N, 2°21′ E and 38 m a.s.l., which is located in the city centre of Paris. This station is approximately 2 km from the LHVP. This site was already equipped with several atmospheric monitoring instruments (including those for CO measurement) and was adapted to use larger instruments than those at the LHVP. An automatic flask sampler (Neubert et al., 2004) and a tunable diode laser (TDL) spectrometer, developed and operated by the Laboratory of Molecular Physics for Atmosphere and Astrophysics (LPMAA, Croizé et al., 2010), were installed for continuous CO_2 and $\delta^{13}CO_2$ measurements. The two inlet lines were located on the roof of the building, 22 m a.g.l.

We used the meteorological parameters of the QualAir station (wind speed and wind direction) as these figures are higher for this station because wind shielding is less important and measurements at this site are more representative than at the LHVP station. During the campaign, wind directions with approximately equal frequency from all four directions and a mean wind speed of 2.7 m s^{-1} have been observed.

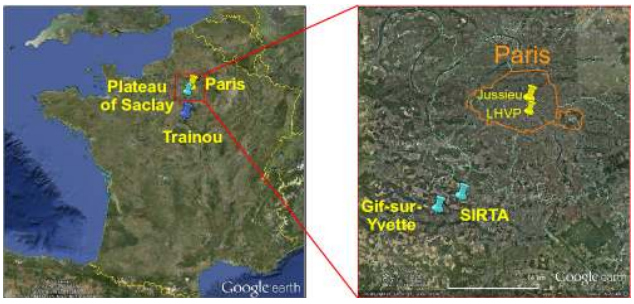

Fig. 1. Location of the different sampling sites.

2.1.2 The Plateau of Saclay

The Plateau of Saclay is a semi-urban flat area that is located approximately 20 km south-west of Paris. The plateau contains atmospheric measurement stations at Gif-sur-Yvette and SIRTA, which are 5 km apart (see Fig. 1). The sites are mainly surrounded by agricultural fields, forests and villages and can be described as suburban.

Gif-sur-Yvette station (Gif station), 48°42′ N, 02°09′ E and 160 m a.s.l., is part of the LSCE and belongs to the RAMCES team. The closest villages and small towns are Saint-Aubin (673 inhabitants) and Gif-sur-Yvette (21 352 inhabitants), which are located 500 m north-west and 1 km south of the station, respectively (Yver et al., 2009). The station is equipped with a gas chromatograph (GC) system that performs continuous measurements of CO_2, CH_4, N_2O, SF_6, CO and H_2 (Pépin et al., 2001; Yver et al., 2009; Lopez et al., 2012). The analytical laboratory is also equipped with an isotope ratio mass spectrometer (IRMS) that is dedicated to the atmospheric measurement of CO_2 isotopes: $\delta^{13}C$ and $\delta^{18}O$ (WMO-GAW, 2005). The inlet lines are located on the roof of the laboratory building, 7 m a.g.l.

The Instrumental Site of Research by Atmospheric Remote Sensing observatory (SIRTA, Haeffelin et al., 2005), located at 48°43′ N, 02°12′ E and 156 m a.s.l., in Palaiseau, is approximately 5 km east of Gif-sur-Yvette station. During the winter campaign, NO_x were monitored by the Interuniversity Laboratory of Atmospheric Systems (LISA).

During the 2010 winter campaign, two primary wind regimes were observed: winds from the north (0–45°) that blew 22 % of the time and transported polluted air masses from Paris, and winds from the west (225–270° wind sector) that also blew 22 % of the time. The mean wind speed in both cases was 5.4 m s^{-1}. During the rest of time, the wind regimes were well distributed among the remaining sectors except for the eastern one (45–90°), which was underrepresented (with winds blowing from that direction less than 3 % of time).

2.1.3 Trainou station

Trainou station (47°57′ N, 02°06′ E, 131 m a.s.l.) is a site located 100 km south of Paris (see Fig. 1) that is mainly surrounded by agricultural fields and forests. The nearest city is Orléans, which is 15 km south-west of the site and has 116 000 inhabitants. Trainou can thus be considered a rural site, especially in comparison to the Paris area. Air inlet lines are located at 5, 50, 100 and 180 m a.g.l. on a television tower (TeleDiffusion de France). Continuous GC analysis for CO_2, CH_4, N_2O, SF_6, CO and H_2 mole fractions have been conducted since 2007 (Messager, 2007; Yver et al., 2010; Lopez et al., 2012). The analysed meteorological variables from the data assimilation system of the European Centre for Medium-Range Weather Forecasts (ECMWF) were used for Trainou station. During the campaign, the station experienced approximately the same wind regimes as Gif-sur-Yvette station, with 24 % of the wind coming from the north-north-east (0–45°) and 25 % of the wind from the west-south-west (225–270°). The mean wind speeds were 4.6 m s^{-1} and 4.3 m s^{-1} for the two sectors, respectively.

2.2 Instrumentation and air sampling strategies

2.2.1 In situ analysers

The cavity ring-down spectrometer (G1302 Picarro, Wastine et al., 2009) that was installed at the LHVP analyses CO_2, CO and water vapour (H_2O) mole fractions with a sampling frequency of 1 Hz. This instrument was calibrated for CO_2 and CO before and after the campaign with four calibration tanks based on the WMO-X2007 scale. During the campaign, two high-pressure cylinders were analysed for 30 min every 10 h. One cylinder was used as a working standard to correct for potential temporal drift by the analyser, and the second cylinder was used as a target gas to evaluate repeatability. During the measurement period, a systematic drift in the CO_2 raw data of 0.08 ppm per month was observed, whereas no significant variation in the CO measurements was detected. After drift corrections for the entire campaign, the target gas showed a repeatability level (1 sigma) of 0.03 ppm for the CO_2 measurements and 10.1 ppb for the CO measurements when 1 min averages were used. Because the ambient air was not dried prior to the CRDS analysis, a water vapour correction for CO_2 was used together with a constant correction (−15 ppb) for CO measurements, which was empirically determined during several weeks of testing in our laboratory in Gif-sur-Yvette (Kaiser et al., 2010).

At Jussieu, a tunable diode laser spectrometer has been installed and is operated by the LPMAA to continuously monitor the atmospheric total CO_2 mole fraction and $\delta^{13}C$ for four consecutive days in February (Croizé et al., 2010). The analysis technique is based on the absorbance correlations between a sealed reference cell and the sample cell. More details regarding the instrumental set-up and calibration strategy used are provided in Croizé et al. (2010). All of the reference and calibration cylinders used in this instrument were calibrated at the central laboratory of LSCE by GC and IRMS.

The two gas chromatographs (Agilent HP-6890 and HP-6890N) located at Gif-sur-Yvette (suburban site) and Trainou (rural site) were optimised for semi-continuous atmospheric measurements. The GC are equipped with two detectors to simultaneously analyse CO_2 and CH_4 with a flame ionisation detector (FID, Messager, 2007) and N_2O and SF_6 with an electron capture detector (ECD, Lopez et al., 2012). In 2006 at Gif-sur-Yvette and in 2009 at Trainou, two Peak Performers (PP1) were coupled to the GC for additional analysis of CO and H_2 using a reduction gas detector (RGD, Yver et al., 2009). In addition to continuous measurements, the GC at Gif-sur-Yvette has been optimised for flask analysis and tank calibration. All of the GC measurements (continuous, flasks and tanks) were calibrated on the WMO-X2007 scale.

The isotope ratio mass spectrometer (Finnigan MAT 252) located at Gif-sur-Yvette measures the isotopic composition of atmospheric CO_2 ($\delta^{13}C$ and $\delta^{18}O$ in CO_2) from flasks (Schmidt et al., 2005). An automated sampling line was set-up according to the "BGC-Airtrap" design as described in Werner et al. (2001) to cryogenically separate CO_2 (along with N_2O) from the other air constituents. The "airtrap" is coupled to the IRMS inlet system and used to analyse the air sampled in the flasks. During the campaign, the IRMS was used for semi-continuous analysis of the atmospheric CO_2 isotopes at Gif-sur-Yvette during a 3 day period. Each analysis sequence consisted of injections of an ambient air standard followed by a target gas and up to 10 flasks, with another ambient air standard injected at the end. The carbon dioxide isotopic data are reported in the δ notation (Eq. 1); R is the ratio of the heavy isotope to the light one. The $\delta^{13}C$ values are referenced to the VPDB scale.

$$\delta = \left(\frac{R_{\text{sample}}}{R_{\text{standards}}} - 1 \right) \times 1000 \quad (1)$$

In addition to CO_2 and CO, NO_x have been monitored at the LHVP and SIRTA stations. NO_x were measured continuously using two chemiluminescent analysers (AC31M, Environment SA) that were operated by the LSCE at the LHVP and by the LISA at SIRTA. A summary of the instrumentation used for this study during the MEGAPOLI campaign is given in Table 1.

2.2.2 Flask sampling strategy and radiocarbon measurements

In addition to continuous measurements, flask sampling was carried out at the LHVP and Jussieu stations. At the LHVP, a manual sampler was used to fill 43 pairs of 1 and 2 L glass flasks. Ambient air was dried using a magnesium perchlorate cartridge. We flushed the flasks for 10 min before pressurisation. The flasks were filled in the morning during the traffic

Table 1. Technologies, models, locations and accuracy of instruments for the analysed species with the respective measurement dates.

Technology	Model	Location	Date	Species and accuracy
CRDS	Picarro G1302	LHVP	15 Jan 2010–19 Feb 2010	CO_2: 0.03 ppm; CO: 10.0 ppb
TDL	SIMCO	Jussieu	8 Feb2010–12 Feb 2010	CO_2: 0.05 ppm; $\delta^{13}C$: 0.15 ‰
GC (FID/ECD)	HP-6890	LSCE Trainou	15 Jan 2010–19 Feb 2010	CO_2: 0.05 ppm; CH_4: 1.0 ppb N_2O: 0.3 ppb; SF_6: 0.05 ppt
GC (RGD)	Peak Performer	LSCE Trainou	15 Jan 2010–19 Feb 2010	CO: 1.0 ppb; H_2: 2.0 ppb
Chemiluminescence	Environment SA AC31M	LHVP SIRTA	15 Jan 2010–15 Feb 2010	NO_x: 10 %
MS	Finnigan MAT 252	LSCE	flasks	$\delta^{13}C$: 0.02 ‰; $\delta^{18}O$: 0.06 ‰
AMS		Boulder (USA)	flasks	$\Delta^{14}C$: 1.4–2.0 ‰

rush hour on six days in February. At Jussieu, we filled 35 flasks of 2.5 L volume every 2 h for two complete days (9–10 and 14–15 February) and during one night (11–12 February). The samples were dried by passing through a water trap maintained in an ethanol bath at −60 °C as described by Neubert et al. (2004). The flasks are automatically flushed for 2 h before pressurisation. All flasks were analysed using a GC and IRMS to provide additional trace gas information and to independently determine the quality of the continuous CRD (CO_2 and CO) and TDL (CO_2, ^{13}C) spectrometer measurements.

We selected 23 flasks (17 from LHVP and 6 sampled at Jussieu) for high-precision $^{14}CO_2$ analysis. Flasks were chosen based on the atmospheric CO_2 mole fraction, and days with large temporal CO_2 gradients were favoured in order to maximise the $^{14}CO_2$ signal with respect to measurement uncertainties (corresponding to $\sim\pm1$ ppm CO_2ff). Compared to the whole campaign, the selected flasks represent well the typical diurnal gradients. The $^{14}CO_2$ samples were prepared at the University of Colorado, Boulder, and measurements were performed via accelerator mass spectrometry (AMS) at the University of California, Irvine, following Turnbull et al. (2007). The radiocarbon values are expressed in Δ notation (Stuiver and Polach, 1977).

As shown in several studies (Levin et al., 2003; Gamnitzer et al., 2006), the amount of $^{14}CO_2$ in atmospheric samples can be used to derive the contribution of fossil fuel CO_2 to the measured atmospheric CO_2 mole fraction. The measured CO_2 mole fraction (CO_2meas) is assumed to consist of a background CO_2 (CO_2bg), a biospheric component (CO_2bio) and a fossil fuel (CO_2ff) component:

$$CO_2\text{meas} = CO_2\text{bg} + CO_2\text{ff} + CO_2\text{bio}. \quad (2)$$

Each component has a characteristic $\Delta^{14}C$ value. $\Delta^{14}C$ff is equal to −1000 ‰ (free of ^{14}C), while $\Delta^{14}C$bg can be measured remotely (or assumed). $\Delta^{14}C$bio is equivalent to $\Delta^{14}C$bg as $\Delta^{14}C$bio includes a correction for mass-dependent fractionation. Equation (3) is then derived as follows:

$$CO_2\text{ff} = CO_2\text{meas} \times \frac{\Delta^{14}\text{Cbg} - \Delta^{14}\text{Cmeas}}{\Delta^{14}\text{Cbg} + 1000}. \quad (3)$$

In Eq. (3), other contributions to the $^{14}CO_2$ budget such as the terrestrial disequilibrium isoflux due to heterotrophic respiration and $^{14}CO_2$ production from nuclear power plants or the reprocessing sector have been neglected. Turnbull et al. (2006) showed that in winter, isoflux corresponds to ~ 0.2 ppm CO_2ff, which is negligible in comparison with the large CO_2ff signal we observe in Paris (see Sect. 3.2). In France, the main production of $^{14}CO_2$ by the nuclear sector is from La Hague (a nuclear waste treatment plant, located approximately 300 km west of Paris), which emits an amount of ^{14}C about 100 times higher than the French nuclear power plants. Using a diffusion model, no influence of air masses from La Hague during the four days of flasks sampling have been observed at Paris.

2.2.3 Comparison of continuous measurements with flasks sampling

The flask results were compared with the corresponding 2 min averages from the continuous analysers. At LHVP, the

mean difference between 36 pairs of flasks and the CRDS analyser data was -0.03 ± 3.33 ppm for CO_2 and -1.9 ± 31.1 ppb for CO, indicating good agreement in both cases. The comparison between the flasks and the TDL spectrometer for the CO_2 mole fraction and $\delta^{13}C$ also indicates good agreement, with mean differences between the flasks and in situ measurements of 0.07 ± 2.33 ppm ($N = 15$) for CO_2 and 0.29 ± 0.20 ‰ ($N = 16$) for $\delta^{13}C$. The substantial standard deviation is likely related to the strong temporal variability in Paris, which often reaches several ppm for CO_2 and 10 ppb for CO in just a few minutes. The 0.29 ‰ mean difference observed in the $\delta^{13}C$ analysis may have been caused by an underestimated correction of the TDL spectrometer measurements. The correction aims to account for the small temperature difference between the atmospheric air and the calibration gas after the atmospheric air has been passed through a cold trap to remove water vapour (Croizé et al., 2010).

The mean mole fraction differences for the CO_2 and CO measurements derived from continuous measurement versus flask sampling are consistent with the WMO-GAW recommendation for background measurements (WMO-GAW, 2009). The objective is to maintain a network intercompatibility level of ±0.1 ppm and ±2 ppb for CO_2 and CO, respectively. The $\delta^{13}C$ figures do not meet the WMO-GAW recommended maximum difference of ±0.01 ‰. The substantial difference is due to instrumental accuracy. However, this difference is not likely to impact the conclusions of this study, which shows that large signals are associated with sampling close to sources in a polluted area.

3 Results and discussion

3.1 The observation of CO_2, CO and NO_x in Paris, at the Plateau of Saclay and at Trainou station

In the Paris region, CO_2 is mainly emitted by anthropogenic sources through the combustion of fossil fuel and biomass (biofuel and wood), although natural sources such as soil respiration also contribute to a degree that remains highly uncertain. Carbon monoxide is often considered as a reliable combustion tracer. It results from fossil fuel and biomass burning and has an atmospheric lifetime of approximately 2 months (assuming an OH value of 10^6 molecules cm^{-3}, Atkinson et al., 2006). Nitrogen oxides are typical markers of traffic exhaust emissions and have a lifetime of approximately 9 h (Atkinson et al., 2006). However, due to its short lifetime, NO_x cannot be transported over long distances and consequently can only be used as tracers for local emissions.

Figure 2 presents the hourly mean CO_2, CO and NO_x mole fractions observed at the LHVP (Paris), at the Plateau of Saclay and at Trainou tower (TR3, 180 m a.g.l. air inlet) from 15 January 2010 to 19 February 2010. The LHVP yielded the highest CO_2, CO and NO_x values, and the data exhibit the largest synoptic variability because the station is close to anthropogenic sources. Trainou yielded the lowest values and synoptic variability, which was expected given that we sampled at 180 m a.g.l. and the rural site likely has weaker local CO_2 and CO sources.

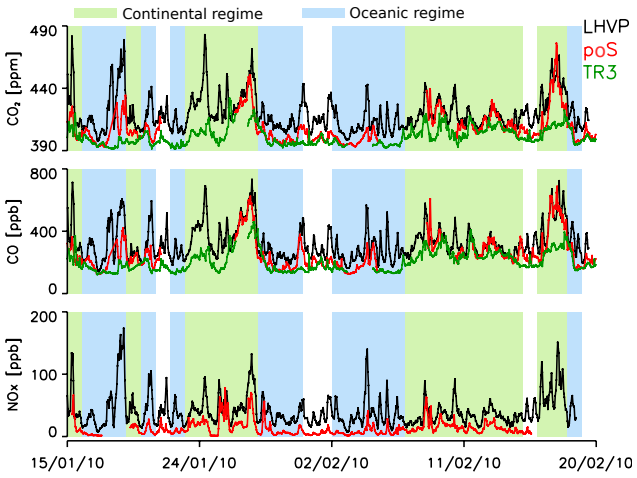

Fig. 2. The CO_2, CO and NO_x mole fractions at the LHVP, Plateau of Saclay (poS) and Trainou 180 m a.g.l. (TR3). Periods during which the air masses originate from the west are highlighted in blue, and periods during which the air masses originate from the east are highlighted in green. No colour is used for the days without a clear air mass origin.

The wind regimes were classified based on back trajectories obtained using the Lagrangian particle dispersion model, FLEXPART (version 8.2), which is described by Stohl et al. (2007). In Fig. 2, the blue areas correspond to times when the air masses that influenced the sites originated from the western sector (180 to 360°). We refer to this as the "oceanic regime" using the MEGAPOLI project nomenclature. The green areas correspond to times when air masses came from eastern Europe (0 to 180°) and crossed Germany or Benelux before arriving at the LHVP, the Plateau of Saclay and Trainou station. We refer to this as the "continental regime". The data collected on days for which air mass back trajectories could not be clearly classified (uncoloured ones) are not considered in the analysis that follows. Figure 3 presents the CO source contributions at LHVP for typical continental (Fig. 3a) and oceanic (Fig. 3b) air masses. Figure 3a and Fig. 3b indicate which grid cells contribute most to our signals. They are also obtained with the FLEXPART model (version 8.2, Stohl et al., 2007) coupled with the EMEP emission inventory (European Monitoring and Evaluation Programme, http://www.emep.int/) for the reference year 2005.

Table 2 summarises the average mole fractions of CO_2, CO and NO_x for the two different regimes. On average, the three sites show higher CO_2 and CO mole fractions during the continental regime. According to a Student's t test, the average mole fractions for the continental and oceanic regimes are statistically distinct at all three sites. Carbon

Table 2. Average of the CO_2, CO and NO_x mole fractions, with their respective standard deviation, as a function of the air mass origin at the LHVP, Plateau of Saclay and Trainou sites from 15 January to 19 February 2010.

Species	CO_2 (ppm)		CO (ppb)		NO_x (ppb)	
Regime	Ocean.	Cont.	Ocean.	Cont.	Ocean.	Cont.
LHVP	414.8 ± 13.4	425.0 ± 14.6	288 ± 98	362 ± 116	39 ± 28	41 ± 24
Plateau of Saclay	401.5 ± 6.9	417.5 ± 14.3	201 ± 62	331 ± 120	12 ± 13	13 ± 11
Trainou	396.8 ± 4.4	405.9 ± 6.7	163 ± 42	249 ± 64		

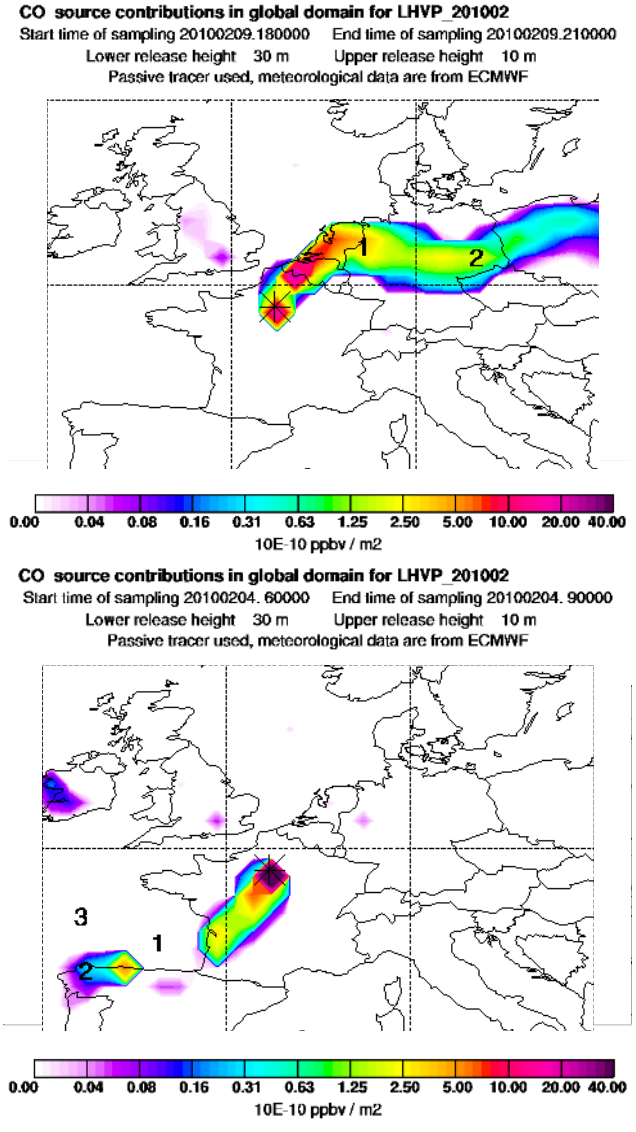

Fig. 3. Maps showing the typical CO source contributions observed for the continental **(a)** and oceanic **(b)** wind regime during the measurement campaign at LHVP.

dioxide and carbon monoxide, with lifetimes of 100 yr and 2 months, respectively, can be transported over longer distances than NO_x can. Thus, higher CO_2 and CO mole fractions are associated with the continental regime because the air masses are progressively charged with pollutants on their trajectory to Paris. When the main wind direction shifts from east (continental) to west (oceanic), a decrease in CO_2 and CO mole fractions is observed. Nitrogen oxides cannot be transported over long distances; thus, at the LHVP and the Plateau of Saclay, NO_x mole fractions are similar for the oceanic and continental regimes.

Figure 4 shows the mean diurnal cycles of CO_2, CO and NO_x at the three stations for both weekdays (in red) and weekends (in black) for the entire measurement period. The mole fractions of trace gases and the mean amplitudes of the diurnal cycles are both smaller at weekends than on weekdays. The mean CO_2, CO and NO_x diurnal cycles show two peaks at LHVP, in the morning (07:00 to 09:00 UTC) and at the end of the afternoon (18:00 to 20:00 UTC). At the Plateau of Saclay, the afternoon peak is weak and is only visible for CO and NO_x. The mean diurnal cycle of the traffic flow in the IdF region during weekdays for the year 2010 is presented along with the NO_x diurnal cycles at the LHVP (Fig. 4). This cycle exhibits the same pattern as the NO_x, CO_2 and CO diurnal cycle, with maxima in the morning and at the end of the afternoon, which suggests the influence of traffic emissions on NO_x measurements. Traffic counts, provided by the Directorate of Ile-de-France roads (DiRIF), are recorded for the main roads of the IdF region. The diurnal cycles of CO_2 and CO at Trainou (180 m a.g.l.) present a single peak at noon on weekend and weekdays primarily reflecting the diurnal dynamics in the planetary boundary layer (PBL) as shown by Lopez et al. (2012) for radon-222 and nitrous oxide.

In Fig. 5, the diurnal cycles of CO_2, CO and NO_x that are recorded at the LHVP are plotted as functions of the air mass origin. The vertical lines are the standard deviation for each hour. As previously explained, the mean concentrations are generally higher when the air masses originate from the east, but the amplitudes of the morning peaks for the three species are similar for the two wind regimes. In contrast, the afternoon peaks in the oceanic wind regimes are more marked for CO_2, CO and NO_x than are those of the continental regime. In the oceanic wind regime, the LHVP is more

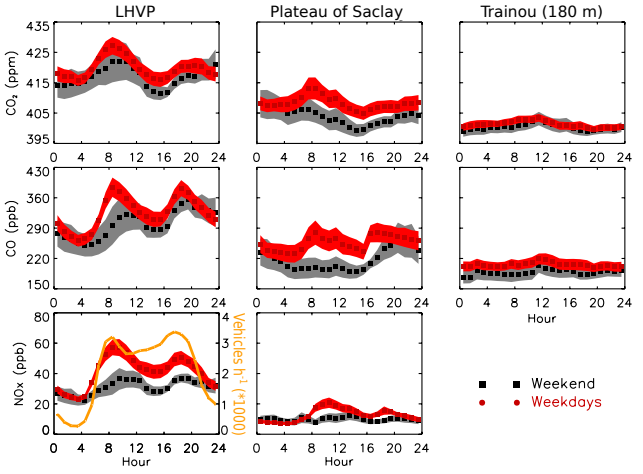

Fig. 4. Mean diurnal cycles of CO_2, CO and NO_x at the LHVP, Plateau of Saclay and Trainou sites for weekend and weekdays with the associated standard deviations. In the NO_x plot for the LHVP, the mean diurnal cycle of vehicle flow during the weekdays for the year 2010 in Ile-de-France is added in orange (DiRIF).

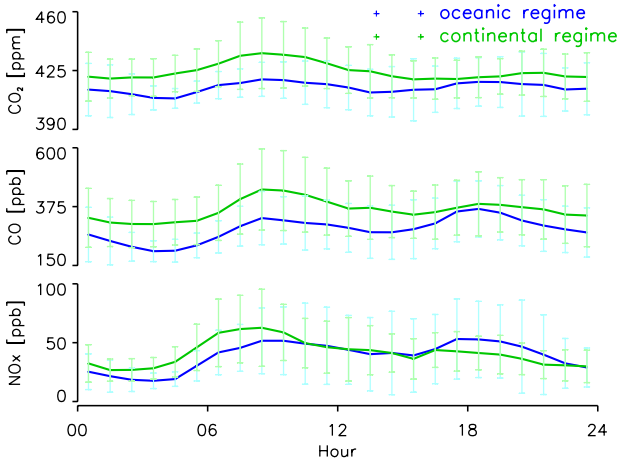

Fig. 5. The CO_2, CO and NO_x diurnal cycles at the LHVP as a function of the air mass regime. The green curves correspond to the continental regime, whereas the blue curves correspond to the oceanic regime. The error bars represent the standard deviation of the mean.

sensitive to local pollution, which increases between 16:00 and 18:00 UTC due to the traffic rush hour and the decrease in the PBL height. The signals decrease at the end of traffic rush hour as the atmosphere is refreshed by relatively clean air masses from the west. This second peak is less marked during the continental regime because the atmosphere is subsequently refreshed by the polluted air masses coming from east of Paris.

At the LHVP, non-methane hydrocarbons including benzene and toluene were monitored during the whole campaign using gas chromatography equipped with an ionisation flame detector (see Gros et al., 2011, for more details). Benzene and toluene have lifetimes of approximately 11 and 2 days, respectively (assuming an OH value of 10^6 molecules cm^{-3}, Atkinson et al., 2006), and are typically emitted by the same sources. The toluene to benzene ratio is therefore often used to determine the photochemical age of an air mass: the lower the ratio, the older the air mass (Roberts et al., 1984; Warneke et al., 2007). This ratio may therefore be used to specify whether the observed pollution originated from a local source or was subject to long-range transport. On 4 and 5 February (oceanic regime), the ratio of toluene to benzene was recorded as approximately 5, whereas on 9 and 10 February (continental regime), the ratio decreased to 2. This result indicates that during the oceanic regime, air masses arriving in Paris were primarily affected by local pollution, whereas during the continental regime, long-range pollution sources were an additional factor.

3.2 Calculating the fossil fuel CO_2 contribution using radiocarbon measurements

In this study, Eq. (3) (see Sect. 2.2.2) is applied to the flasks sampled at the LHVP and Jussieu station to quantify the contribution of fossil fuel CO_2 to the ambient air in Paris. The background value of Δ^{14}Cbg is derived from $^{14}CO_2$ measurement at Mace Head (Ireland, 53°19′ N, 9°54′ W, 25 m a.s.l.), which is considered a background site for Europe. In February 2010, the monthly mean $^{14}CO_2$ and CO_2 values at Mace Head (wind selected for the oceanic sector, Bousquet et al., 1996) were 43.7 ‰ (I. Levin, personal communication, 2011) and 393.5 ppm, respectively. The analysis of the flasks yielded Δ^{14}Cmeas between −54.04 and +15.59 ‰ and a resulting CO_2ff contribution of 10.9 to 41.9 ppm relative to the background air at Mace Head.

Figure 6 presents an example of a typical measurement day, 4 February 2010, at the LHVP. The 1 min averaged CO_2 mole fractions obtained via continuous measurement are plotted in orange, and the CO_2 mole fractions obtained from the flask measurements are indicated with red crosses. The background CO_2 mole fraction at Mace Head during the maritime background conditions (Bousquet et al., 1996) for February 2010 is plotted in blue.

Combining the CO_2 and $\Delta^{14}CO_2$ measurements from the individual flask samples permits us to determine the contribution of CO_2ff and CO_2bio to the observed CO_2 mole fraction following Eq. (2): see Fig. 6. Fossil fuel CO_2 increases by 22.7 ppm from 07:15 to 08:15 UTC to reach a maximum of 41.9 ppm. Subsequently, we observe a small decrease until 12:00 UTC followed by a strong decrease (17.0 ppm) to 17.2 ppm at 13:00 UTC. The NO_x cycle (not shown) follows the same pattern, suggesting that local traffic contributes to

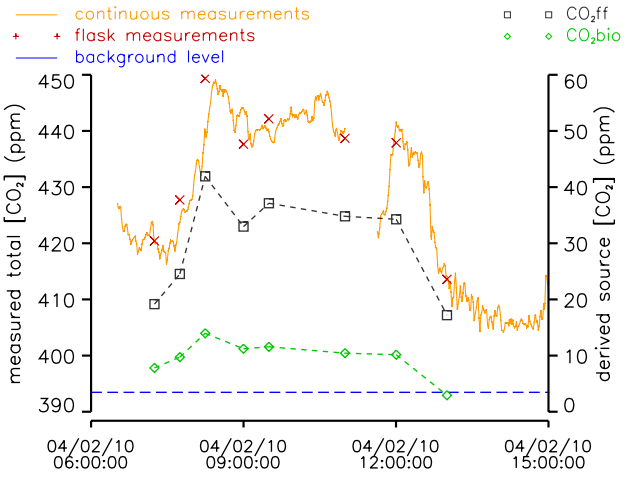

Fig. 6. A comparison between the continuous measurements for CO_2 (in orange) and the data obtained using flask sampling (red crosses) at the LHVP site are presented for 4 February 2010 on the left axis. We added the background level of CO_2 as measured at Mace Head (Ireland), which is represented by the blue horizontal dashed line. The figures for CO_2ff and CO_2bio, as derived from flask sampling, are represented on the right axis by the black and green curves, respectively. The left and right axes have the same CO_2 amplitude.

the CO_2ff signal in the centre of Paris. The morning CO_2ff increase is due to the morning rush hour, and the subsequent decrease indicates the reduction in traffic as well as the PBL development. The figures for CO_2bio are lower (0–10 ppm) and exhibit less variation than those of CO_2ff. The same diurnal cycles are observed for CO_2ff and CO_2bio for the four sampling days at the LHVP and the single sampling day at Jussieu. Table 3 summarises the daily averages for CO_2ff and CO_2bio for each sampling day. The fossil fuel CO_2 enhancement with respect to the background varies from 16.2 to 32.8 ppm, and the biospheric CO_2 contribution varies from 4.5 to 10.2 ppm. The differences in the CO_2ff and CO_2bio mole fractions at the LHVP and Jussieu sites as they were observed on 10 February are related to the sampling period and location.

The contributions of the two CO_2 sources (fossil fuel and biogenic) to the CO_2meas variability show that the majority of this variability is due to the injection of CO_2ff into the atmosphere. On average, 77 % of the observed signal is caused by CO_2ff (Table 3), mainly from road traffic, heating and the residential sectors. However, despite Paris being a megacity, the biospheric contribution of CO_2 fluxes was significant (23 % on average), even in winter.

This biospheric contribution of approximately 23 % can be attributed not only to net plant and soil respiration but also to the use of biofuel and to human respiration, which cannot be identified using $^{14}CO_2$ measurements because these sources have been fixed or metabolised recently and have isotopic signatures that are similar to that of the ambient atmosphere. In this paragraph we attribute a percentage to the different biospheric sources in Paris using emission inventories and literature values. According to an AirParif emission inventory, CO_2 emissions from wood burning used for residential heating contribute less than 1 % of the total emissions in Paris and likely do not contribute significantly to the observed CO_2bio enhancement. By 2010, the biofuel ratios in gasoline and diesel increases to approximately 7 % in France, which suggests that road traffic sources contribute significantly to the CO_2bio results. In France, most of the biofuel is produced from rape, wheat and sugar beats (C3 plants), having a $\delta^{13}C$ signature of approximately -28 ‰. AirParif estimates that the contribution of CO_2 from traffic is 17 % of the total fossil fuel CO_2 emissions for January 2008 after the emissions associated with biofuel in gasoline and diesel have been removed. According to our mean results for CO_2ff and CO_2bio as presented in Table 3, this contribution corresponds to an average CO_2ff of 5 ppm from traffic. Because gasoline and diesel contain up to 7 % biofuel, the CO_2bio enhancement due to traffic sources is 0.4 ppm, or approximately 12 % of the CO_2bio in Paris during the winter. A study by Turnbull et al. (2011) determined that the use of biofuels contributed up to 1 ppm of the positive CO_2bio signal when gasoline contained approximately 8 % ethanol in California.

A study by Ciais et al. (2007) shows that CO_2 emissions from human respiration in densely populated cities can reach 20 % of fossil fuel CO_2 emissions. Koerner and Klopatek (2002) show that human respiration is 500 kg CO_2 per year per person on average. With a population of 2.2 million in the centre of Paris, human respiration in the centre may be responsible for CO_2 emissions of approximately 1100 kt yr^{-1}. By comparing this value to the reported fossil fuel CO_2 emissions of 7218 kt for the year 2005 in Paris reported by AirParif, human respiration contributes 15 % of the CO_2ff emissions; this percentage is similar to the value reported in Ciais et al. (2007). Human respiration should be responsible for approximately 4 ppm of the CO_2 enhancement, and may therefore account for approximately 50 % of the CO_2bio calculated.

Here we can conclude that the biogenic sources can be attributed to 38 % of the net plant and soil respiration, 50 % to human respiration and 12 % to the use of biofuel. These values are only representative for our sampling sites at the LHVP and Jussieu in February 2010.

3.3 Separation of fossil fuel CO_2 sources using $\delta^{13}C$ measurements

Several studies (Zondervan and Meijer, 1996; Meijer et al., 1996; Djuricin et al., 2010) have used ^{13}C / ^{12}C ratios in combination with ^{14}C measurements to quantify the fractions of emissions by different fossil fuel sources. Tans (1981) estimated that the release of CO_2 via anthropogenic combustion implies average worldwide $\delta^{13}C$ emissions for natural

Table 3. CO_2ff and CO_2bio emissions with their respective contributions derived at the LHVP and at Jussieu.

Site	No. of flasks	Date	CO_2 enhancement (ppm)		Respective distribution (%)	
			CO_2ff	CO_2bio	CO_2ff	CO_2bio
LHVP	8	4 Feb 2010	30.2	9.7	76	24
LHVP	3	5 Feb 2010	16.2	4.5	78	22
LHVP	3	9 Feb 2010	26.6	10.2	72	28
LHVP	3	10 Feb 2010	32.8	8.6	79	21
Jussieu	6	10 Feb 2010	25.1	6.9	78	22

gas (δ^{13}Cgas), liquid (δ^{13}Cliq) and solid (δ^{13}Csol) fuel of -41.0, -26.5 and -24.1 ‰, respectively. More recently, Andres et al. (2000) shown that δ^{13}C signatures depend on the geographic origin of fossil fuels and can range from -19 to -35 ‰ for liquids and from -20 to -100 ‰ for natural gas. A study by Widory and Javoy (2003) determined δ^{13}C from the main pollution source in Paris by directly measuring exhaust gases. The authors determined that the mean δ^{13}C source ratio for natural gas, liquid fuel and coal is -39.1 ± 1.1, -28.9 ± 0.4 and -24.8 ± 0.4 ‰, respectively. Based on the atmospheric δ^{13}C and CO_2 measurements, we estimate the signatures of the main δ^{13}C sources, using a Keeling plot (Keeling, 1958, 1961; Pataki et al., 2003) for the daily observations. Assuming mass conservation and following Eq. (2) (see Sect. 2.2.2), we derive Eq. (4), where CO_2s represents the sum of the CO_2 sources (i.e. $CO_2s = CO_2ff + CO_2bio$). Combining Eqs. (2) and (4), we obtain Eq. (5). We compute the relationship between δ^{13}Cmeas and the inverse mole fraction of the corresponding CO_2 using a least-squares method following Pataki et al. (2003). The intercept corresponds to the mean signature of the source: δ^{13}Cs (i.e. the last term of Eq. 5). These values have been corrected for biospheric δ^{13}C emission, assuming that $\delta^{13}Cbio = -24.7$ ‰ (Bakwin et al., 1998), resulting in δ^{13}Cff.

$$\delta^{13}\text{Cmeas} \times \text{CO}_2\text{meas} = \delta^{13}\text{Cbg} \times \text{CO}_2\text{bg} + \delta^{13}\text{Cs} \times \text{CO}_2\text{s} \quad (4)$$

$$\delta^{13}\text{Cmeas} = \frac{\text{CO}_2\text{bg} \times (\delta^{13}\text{Cbg} - \delta^{13}\text{Cs})}{\text{CO}_2\text{meas}} + \delta^{13}\text{Cs} \quad (5)$$

Based on the data from the flasks sampled during the entire measurement period, δ^{13}Cff at LHVP and Jussieu was equal to -36.1 ± 2.7 ‰ and -36.2 ± 1.1 ‰, respectively, where the errors are given by the uncertainty in the intercept from Eq. (5). According to AirParif, the use of coal in the Paris region accounts for less than 1 % of the total anthropogenic CO_2 emission; thus, we will neglect this source. Using the δ^{13}Cgas and δ^{13}Cliq values measured by Widory and Javoy (2003) and the δ^{13}Cff source values from the Keeling plots yielded percentages of 70 ± 6 % for natural gas and 30 ± 3 % for liquid fuel. The emission inventory for Paris for 2008 that was provided by AirParif (described in Sect. 3.5) estimates the contribution of natural gas to be 37 % of the total CO_2 emissions.

We surmise that the higher ratio of gas consumption derived using the atmospheric method (70 ± 6 %) compared to the AirParif emission inventory (37 %) likely arose from the spatial separation of automotive and residential sources and the lack of complete mixing prior to the sampling at our sampling location. We conducted our sampling during only a few days in winter, whereas the fraction provided by AirParif takes into account data from the entire year. We expected a higher fraction of gas consumption during the winter due to enhanced heating use.

Pataki et al. (2006) conducted $\delta^{13}CO_2$ continuous measurements over Salt Lake City (Utah, USA) during the early winter of 2004–2005. Using the same approach as presented in this section, they found a natural gas contribution between 30 and 40 % during morning rush hour and 60 and 70 % at pre-dawn. Newman et al. (2008) analysed $\delta^{13}CO_2$ in flasks for the years 2002–2003 in Pasadena (Los Angeles Basin, California, USA). They found a Keeling intercept of -29.9 ± 0.2 ‰, which is less depleted than our value (-36.1 ± 2.7 ‰). This shows a stronger annual influence of liquid fuel use in the total CO_2 emission in Pasadena, compared with the winter in Paris. Administration of the US Department of Energy indicates that that 62 % of the state of California's energy from fossil fuel is from petroleum products and 37 % from natural gas.

3.4 Constructing a continuous time series of fossil fuel CO_2

Precise $^{14}CO_2$ measurements are difficult to perform and are only possible on discrete samples. Therefore, there are no direct methods of obtaining a continuous record of fossil fuel CO_2. To derive such a record for the entire campaign (defined here as $FFCO_2$), we used two potential proxies: CO (see Gamnitzer et al., 2006; Levin and Karstens, 2007) and NO_x. To our knowledge, this is the first time that NO_x are used as proxy to derive the CO_2 fossil fuel contribution. Both tracers are known to be typical proxies for fossil fuel combustion, but the emission ratios with respect to CO_2ff vary as a function of the combustion source. The daily ratios of each selected proxy of CO_2ff for the four days when we took ^{14}C

Table 4. $\frac{CO}{CO_2ff}$ (R_{CO}) and $\frac{NO_x}{CO_2ff}$ (R_{NO_x}) ratios with their respective coefficients of determination (r^2) and the number of points used for each sampled day and the corresponding values used for each regime (3 last lines).

Date	Wind regime	R_{CO}	R_{NO_x}	No. of points used
4 Feb 2010	oceanic	11.5 ($r^2 = 0.75$)	3.7 ($r^2 = 0.89$)	8
5 Feb 2010	oceanic	14.5 ($r^2 = 0.90$)	4.3 ($r^2 = 0.96$)	3
9 Feb 2010	continental	9.2 ($r^2 = 0.97$)	1.1 ($r^2 = 0.92$)	3
10 Feb 2010	continental	7.9 ($r^2 = 1$)	2.1 ($r^2 = 0.91$)	3
	oceanic regime	13.0	4.0	11
	continental regime	8.5	1.6	6
	not clearly defined regime	10.8	2.8	

measurements at the LHVP site were used to construct the $FFCO_2$ curve. To compute the ratios R_{CO} and R_{NO_x}, defined here as $\frac{CO}{CO_2ff} \times 1000$ and $\frac{NO_x}{CO_2ff} \times 1000$, we subtracted the background mole fraction from the ambient measurements. To ensure consistency, we chose to use the background CO mole fraction from the winter 2010 at Mace Head, which was equal to 121 ppb (Derwent et al., 2001, http://agage.eas.gatech.edu/Stations/macehead.htm). For NO_x background, we used a value of zero because of its short lifetime (close to 9 h). The CO_2ff terms do not take into account the contribution of CO_2 from biofuel use. To determine the $FFCO_2$ values, Eqs. (6) and (7) were used.

$$FFCO_2(CO) = \frac{CO - CObg}{R_{CO}} \quad (6)$$

$$FFCO_2(NO_x) = \frac{NO_x}{R_{NO_x}} \quad (7)$$

The emissions ratios for each of the four days of measurements at the LHVP are presented in Table 4 along with their respective coefficients of determination (r^2). We observe that the ratios are functions of the wind regime (Table 4), with higher values on 4 and 5 February (oceanic regime) than on 9 and 10 February (continental regime). An average ratio for each air mass regime is applied to the appropriate segments of the continuous measurements to compute the $FFCO_2$ for each regime. For the few days without clearly identified air mass origin, we use the mean value from the two synoptic situations (Table 4).

In the upper panel of Fig. 7, we present the two curves inferred from R_{CO} and R_{NO_x}: $FFCO_2(CO)$ and $FFCO_2(NO_x)$, respectively. The estimated $FFCO_2$ is greater during the continental wind regime: up to 80 ppm at three different times. In contrast, during the oceanic regime, the $FFCO_2$ mole fractions never exceed 40 ppm. At the bottom of Fig. 7, the $FFCO_2(CO)$ and $FFCO_2(NO_x)$ mean diurnal cycles are plotted. These plots show the same pattern: a peak during the morning in the rush hour and a second peak at the end of afternoon. The $FFCO_2(CO)$ and $FFCO_2(NO_x)$ mean mole fractions are 20.6 and 18.7 ppm, respectively. Differences are

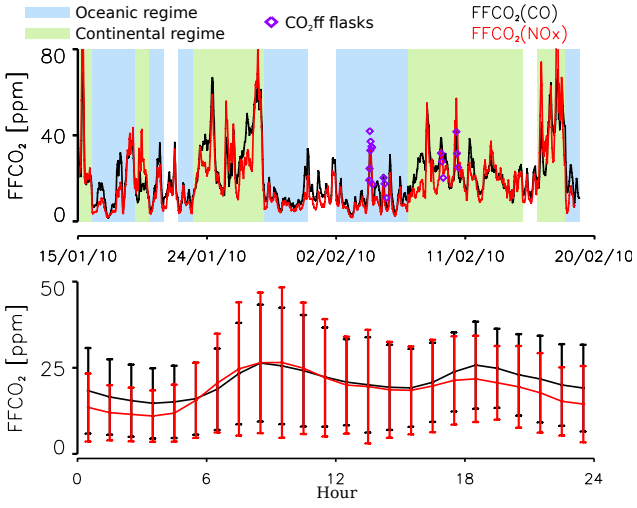

Fig. 7. Top: time series for $FFCO_2$ during the MEGAPOLI campaign calibrated using CO and NO_x as proxies. The purple rhombuses correspond to the CO_2ff from the flasks sampling. Periods during which the air masses originate from the west are highlighted in blue, and periods during which the air masses originate from the east are highlighted in green. No colour is attributed on the days without a clear air mass origin (see Fig. 2). Bottom: mean diurnal cycles of $FFCO_2(CO)$ in black and $FFCO_2(NO_x)$ in red at the LHVP station from 15 January 2010 to 19 February 2010.

observed during the evening and over night (from 17:00 until 06:00 UTC) because of the short lifetime of NO_x relative to the lifetime of CO.

A study by Vogel et al. (2010) shows that R_{CO} has a diurnal cycle because anthropogenic CO_2 (and CO) fluxes are subject to strong diurnal variation. During the winter, the authors found a peak-to-peak amplitude of 8 ppb ppm^{-1}, with the lowest ratio at 08:00 UTC and the highest at 18:00 UTC. We assume a constant ratio during the day in this study.

Table 5. CO_2 contribution estimates by different inventories for the three main emission sectors. From the emission values, we computed the total ratios R_{CO} and R_{NO_x} and also the ratios by sectors.

	Emission (%)			R_{CO}				R_{NO_x}			
	Road	Resid.	Ind.	Total	Road	Resid.	Ind.	Total	Road	Resid.	Ind.
CITEPA											
2005	31	24	24	16.0	11.1	16.5	18.1	3.5	5.9	1.1	2.0
2008	31	24	24	14.7	7.4	15.8	17.6	3.1	5.4	1.1	1.8
2010	31	25	23	13.4	5.3	14.5	17.5	2.9	4.8	1.1	1.7
EDGAR 4.2 France (2008)	32	24	27	8.1	4.4	15.1	0.8	2.7	3.5	1.4	2.2
EDGAR 4.2 Paris (2008)	73	12	9	4.3	5.4	1.0	0.9	3.9	4.3	2.0	4.0
IER Paris (2005)	36	45	15	14.6	12.8	19.8	0.4	3.0	4.3	1.2	3.6
AirParif Paris (Jan. 2008)	30	63	7					2.1	4.1	1.2	1.5

3.5 Comparison of R_{CO} and R_{NO_x} ratios with emission inventories

In this section, we compare the R_{CO} and R_{NO_x} emission ratios measured in Paris with those derived from emission inventories. Four different emission inventories are presented with different spatial and temporal resolutions. The reference years for the inventories vary from 2005 to 2010, which makes it difficult to compare the ratios directly. For France as a whole, CITEPA has calculated the GHG emissions on a yearly basis since 1960. In addition, AirParif provides a regional inventory for the IdF with a spatial resolution of 1 km × 1 km. AirParif assessed the CO_2 and NO_x emissions with a 1 h time resolution for three typical days (weekdays, Saturdays and Sundays) in January 2008. The Institute for Energy Economics and the Rational Use of Energy (IER, 2005) has provided a European inventory with a resolution of 1 min × 1 min for France for the year 2005. EDGAR 4.2 is a global inventory of GHG emissions and has reported annual values for France since 1970. EDGAR 4.2 also provides a gridded version with a resolution of 0.1 ° × 0.1 °for the reference year 2008 (Olivier et al., 2001; Olivier and Berdowsky, 2001). The spatial resolution of IER and AirParif allowed for us to extract the exact grid cells that corresponded to Paris, whereas for EDGAR 4.2, we chose the grid cell that included most of the Paris area.

The total ratios for each inventory are presented in Table 5 for different reference years and spatial and time resolutions. For France as a whole, CITEPA estimates a higher total R_{CO} ratio than does EDGAR 4.2, whereas the total ratios are similar for R_{NO_x}. For Paris, EDGAR 4.2 shows much lower total R_{CO} ratios (4.3) than does the IER inventory (14.6). The R_{NO_x} ratios vary substantially across the different emission inventories; they are 3.9 (EDGAR 4.2), 3.0 (IER) and 2.1 (AirParif). These differences are due to discrepancies in the spatial source distribution for Paris and to the different ratios used for the same source sectors in different inventories. These large differences between inventories suggest that more work needs to be done to provide more consistent estimates.

In Table 5, we also summarised the percentage contributions of the three main source sectors (road transport, residential and industry) as well as the R_{CO} and R_{NO_x} ratios for the different sectors for the different inventories. For France as a whole, the R_{CO} and R_{NO_x} ratios stayed fairly constant between 2005 and 2010 except for the road transport ratio. The R_{CO} ratio for road transport decreased by a factor of 2 in five years. This decrease is primarily a function of the environmental policy applied to road vehicles since 1970 and is also an effect of the adoption and improvement of catalytic converters for vehicles since 1993, which has reduced NO_x and particularly CO emissions.

We compared the ratios determined using our top-down atmospheric approach (Table 4) with the available inventories (Table 5). We focus first on the R_{CO} ratio and then on the R_{NO_x} ratio. During oceanic regimes, our mean R_{CO} ratio of 13 is similar to the ratios from IER and CITEPA (Table 5). These high ratios are representative of the residential sector. This result is consistent with the ratio of benzene to toluene that we found in Sect. 3.1, which indicates that our samples are sensitive to local emissions during the oceanic regime. Our R_{CO} ratio for the continental regime is 8.5 and lies between the IER and CITEPA estimates and those of EDGAR 4.2. According to the AirParif inventory, the north and north-eastern areas of Paris have relatively significant CO_2 emissions from industrial sources

(approximately 20 % of anthropogenic CO_2) compared with southern Paris (less than 5 % of anthropogenic CO_2). This result is in agreement with the ratio that we found for the continental regime, which indicates that the contribution of the road transport and industry sectors, which have low R_{CO} ratios, are stronger. Moreover, the ratio of benzene to toluene during this regime indicated that long-range transport had occurred, which would have permitted the emissions from Benelux and Germany to have a greater influence. These are industrialised areas that are characterised by relatively low R_{CO} ratios relative to those of France (Gamnitzer et al., 2006). We noticed that EDGAR 4.2 found a much lower R_{CO} in Paris than did other inventories and that this figure was also much lower than our estimate. This difference is most likely due to the low R_{CO} ratio of 1.0 for the residential sector for the Paris grid cell relative to the high value of 15.1 for France.

Because of its short lifetime, the R_{NO_x} ratio is less sensitive to contributions from different sources. Nevertheless, the ratios we found are within the range of the inventory estimates. During the continental regime, NO_x were destroyed during transport over the continent, which leads to lower R_{NO_x} values. In the oceanic regime, the high ratios reflect the contribution of the road transport sector near the station. The ratios derived with our atmospheric approach for the different regimes agree well with the emission inventories given the uncertainties of the different approaches.

4 Conclusions

This pilot study has demonstrated that measurement of CO_2, CO and NO_x mole fractions together with isotopic CO_2 measurements can help to better quantify the fossil fuels component in cities. Radiocarbon measurements using flask sampling allowed for us to directly derive the fossil fuel CO_2 mole fraction in Paris, which was approximately 20 ppm (on average), in February 2010. Of the total CO_2 enhancement in Paris during this period, 77 % can be attributed to anthropogenic sources (CO_2ff) and 23 % to biospheric sources (CO_2bio). Using values from the literature, we estimated that half of these biospheric emissions are due to human respiration and that the other half are due to soil respiration (38 %) and the use of biofuel in gasoline and diesel (12 %).

Making use of $\delta^{13}C$ measurements, we were able to determine the contributions of natural gas and liquid fuel to anthropogenic CO_2 emissions, which amounted to 70 % and 30 %, respectively. This estimation was possible in Paris because there are only two sources of fossil fuel emissions; the use of coal can be neglected because it produces less than 1 % of the total CO_2 emission. This calculation would be even more powerful if we could reduce the errors generated by the isotopic source signature of natural gas, which varies according to the supply of natural gas (i.e. whether it originates in Siberia or the North Sea). During future campaigns, it would be helpful to measure the source signature of natural gas from the gas supply network on a regular basis.

Carbon monoxide and nitrogen oxides, which were monitored continuously, were successfully used as proxies to determine the anthropogenic CO_2 emissions over the entire campaign. These proxies have been calibrated against the $\frac{CO}{CO_2ff}$ and $\frac{NO_x}{CO_2ff}$ ratios. We determined that the ratios change as a function of the air mass origin. Therefore, it was possible to use different ratios for the proxies depending on the air mass regime. The data for the $\frac{CO}{CO_2ff}$ and $\frac{NO_x}{CO_2ff}$ ratios are consistent with the information from the inventories although there are sizeable variations across the inventories themselves. According to these inventories, during the oceanic regime, we are more sensitive to the emissions from the residential sector, where the $\frac{CO}{CO_2ff}$ ratio is high. During the continental regime, that ratio decreases, showing increasing influence of the road transport and industrial sectors.

Acknowledgements. We thank the MEGAPOLI project (funded by the European Union's Seventh Framework Programme FP/2007-2011) that allowed us to place our instruments at LHVP during the winter campaign 2010. We used NO_x and VOCs data from the MEGAPOLI Database. We thank François Truong, Cyrille Vuillemin and Vincent Bazantay from LSCE/RAMCES for maintaining the instrumentation during the campaign and performing the flask analysis. We thank Ingeborg Levin for providing ^{14}C measurement at Mace Head as well as Yao Té and Pascal Jeseck for the meteorological data for the Jussieu site. We want to thank Claude Camy-Peyret for his occasional help during the campaign with TDL spectrometer and Laurence Croizé for the instrumental development. We also thank Balendra Thiruchittampalam for the helpful discussions about IER inventory. This work was supported partly by the ANR-CO_2-MegaParis project, GHG-Europe, CNRS and CEA.

Edited by: C. Reeves

The publication of this article is financed by CNRS-INSU.

References

Andres, R. J., Marland, G., Boden, T., and Bischof, S.: Carbon dioxide emissions from fossil fuel consumption and cement manufacture, 1751–1991, and an estimate of their isotopic composition and latitudinal distribution, The carbon cycle, 62, 53–62, New York, 2000.

Atkinson, R., Baulch, D. L., Cox, R. A., Crowley, J. N., Hampson, R. F., Hynes, R. G., Jenkin, M. E., Rossi, M. J., Troe, J., and IUPAC Subcommittee: Evaluated kinetic and photochemical data for atmospheric chemistry: Volume II – gas phase reactions of organic species, Atmos. Chem. Phys., 6, 3625–4055, doi:10.5194/acp-6-3625-2006, 2006.

Bakwin, P. S., Tans, P. P., White, J. W. C., and Andres, R. J.: Determination of the isotopic $^{13}C/^{12}C$ discrimination by terrestrial biology from a global network of observations, Global Biogeochem. Cy., 12, 555–562, 1998.

Bousquet, P., Gaudry, A., Ciais, P., Kazan, V., Monfray, P., Simmonds, P. G., Jennings, S., and O'Connor, T.: Atmospheric CO_2 concentration variations recorded at Mace Head, Ireland, from 1992 to 1994, Phys. Chem. Earth, 21, 477–481, 1996.

Bousquet, P., Peylin, P., Ciais, P., Le Quéré, C., Friedlingstein, P., and Tans, P. P.: Regional changes in carbon dioxide fluxes of land and oceans since 1980, Science, 290, 1342–1346, 2000.

Bousquet, P., Ciais, P., Miller, J. B., Dlugokencky, E. J., Hauglustaine, D. A., Prigent, C., Van der Werf, G. R., Peylin, P., Brunke, E. G., Carouge, C., Langenfelds, R. L., Lathiere, J., Papa, F., Ramonet, M., Schmidt, M., Steele, L. P., Tyler, S. C., and White, J.: Contribution of anthropogenic and natural sources to atmospheric methane variability, Nature, 443, 439–443, 2006.

Ciais, P., Bousquet, P., Freibauer, A., and Naegler, T.: Horizontal displacement of carbon associated with agriculture and its impacts on atmospheric CO_2, Global Biogeochem. Cy., 21, GB2014, doi:10.1029/2006GB002741, 2007.

CITEPA: Rapport national d'inventaire pour la France au titre de la convention cadre des Nations Unies sur les changements climatiques et du protocole de Kyoto, 2012.

Croizé, L., Mondelain, D., Camy-Peyret, C., Janssen, C., Lopez, M., Delmotte, M., and Schmidt, M.: Isotopic composition and concentration measurements of atmospheric CO_2 with a diode laser making use of correlations between non-equivalent absorption cells, Appl. Phys. B-Lasers O., 101, 411–421, 2010.

Derwent, R. G., Ryall, D. B., Jennings, S. G., Spain, T. G., and Simmonds, P. G.: Black carbon aerosol and carbon monoxide in European regionally polluted air masses at Mace Head, Ireland during 1995–1998, Atmos. Environ., 35, 6371–6378, 2001.

Djuricin, S., Pataki, D. E., and Xu, X.: A comparison of tracer methods for quantifying CO_2 sources in an urban region, J. Geophys. Res., 115, D11303, doi:10.1029/2009JD012236, 2010.

Dolgorouky, C., Gros, V., Sarda-Esteve, R., Sinha, V., Williams, J., Marchand, N., Sauvage, S., Poulain, L., Sciare, J., and Bonsang, B.: Total OH reactivity measurements in Paris during the 2010 MEGAPOLI winter campaign, Atmos. Chem. Phys., 12, 9593–9612, doi:10.5194/acp-12-9593-2012, 2012.

Duren, R. M. and Miller, C. E.: Measuring the carbon emissions of megacities, Nature Climate Change, 2, 560–562, 2012.

Gamnitzer, U., Karstens, U., Kromer, B., Neubert, R. E. M., Meijer, H. A. J., Schroeder, H., and Levin, I.: Carbon monoxide: A quantitative tracer for fossil fuel CO_2, J. Geophys. Res, 111, D22302, doi:10.1029/2005JD006966, 2006.

Gros, V., Gaimoz, C., Herrmann, F., Custer, T., Williams, J., Bonsang, B., Sauvage, S., Locoge, N., d'Argouges, O., Sarda-Estève, R., and Sciare, J.: Volatile organic compounds sources in Paris in spring 2007. Part I: Qualitative analysis, Environ. Chem., 8, 74–90, 2011.

Haeffelin, M., Barthès, L., Bock, O., Boitel, C., Bony, S., Bouniol, D., Chepfer, H., Chiriaco, M., Cuesta, J., Delanoë, J., Drobinski, P., Dufresne, J.-L., Flamant, C., Grall, M., Hodzic, A., Hourdin, F., Lapouge, F., Lemaître, Y., Mathieu, A., Morille, Y., Naud, C., Noël, V., O'Hirok, W., Pelon, J., Pietras, C., Protat, A., Romand, B., Scialom, G., and Vautard, R.: SIRTA, a ground-based atmospheric observatory for cloud and aerosol research, Ann. Geophys., 23, 253–275, doi:10.5194/angeo-23-253-2005, 2005.

Hammer, S. and Levin, I.: Seasonal variation of the molecular hydrogen uptake by soils inferred from continuous atmospheric observations in Heidelberg, southwest Germany, Tellus B, 61, 556–565, 2009.

Healy, R. M., Sciare, J., Poulain, L., Kamili, K., Merkel, M., Müller, T., Wiedensohler, A., Eckhardt, S., Stohl, A., Sarda-Estève, R., McGillicuddy, E., O'Connor, I. P., Sodeau, J. R., and Wenger, J. C.: Sources and mixing state of size-resolved elemental carbon particles in a European megacity: Paris, Atmos. Chem. Phys., 12, 1681–1700, doi:10.5194/acp-12-1681-2012, 2012.

Hirsch, A. I., Michalak, A. M., Bruhwiler, L. M., Peters, W., Dlugokencky, E. J., and Tans, P. P.: Inverse modeling estimates of the global nitrous oxide surface flux from 1998–2001, Global Biogeochem. Cy., 20, GB1008, doi:10.1029/2004GB002443, 2006.

IER: Emission data, http://carboeurope.ier.uni-stuttgart.de (last access: January 2013), 2005.

Kaiser, C., Schmidt, M., Lavric, J. V., Laurent, O., Vuillemin, C., Yver, C., and Ramonet, M.: Evaluation of five CO analysers , Tech. rep., LSCE-CEA-CNRS-IPSL, Gif-sur-Yvette, 2010.

Keeling, C. D.: The concentration and isotopic abundances of atmospheric carbon dioxide in rural areas, Geochim. Cosmochi. Ac., 13, 322–334, 1958.

Keeling, C. D.: The concentration and isotopic abundances of carbon dioxide in rural and marine air, Geochim. Cosmochim. Ac., 24, 277–298, 1961.

Koerner, B. and Klopatek, J.: Anthropogenic and natural CO_2 emission sources in an arid urban environment, Environ. Pollut., 116, Supplement 1, S45–S51, doi:10.1016/S0269-7491(01)00246-9, 2002.

Levin, I. and Karstens, U.: Inferring high-resolution fossil fuel CO_2 records at continental sites from combined $^{14}CO_2$ and CO observations, Tellus B, 59, 245–250, 2007.

Levin, I., Kromer, B., Schmidt, M., and Sartorius, H.: A novel approach for independent budgeting of fossil fuel CO_2 over Europe by $^{14}CO_2$ observations, Geophys. Res. Lett., 30, 2194, doi:10.1029/2003GL018477, 2003.

Lopez, M., Schmidt, M., Yver, C., Messager, C., Worthy, D., Kazan, V., Ramonet, M., Bousquet, P., and Ciais, P.: Seasonal variation of N_2O emissions in France inferred from atmospheric N_2O and ^{222}Rn measurements, J. Geophys. Res., 117, D14103, doi:10.1029/2012JD017703, 2012.

Meijer, H. A. J., Smid, H. M., Perez, E., and Keizer, M. G.: Isotopic characterisation of anthropogenic CO_2 emissions using isotopic and radiocarbon analysis, Phys. Chem. Earth, 21, 483–487, 1996.

Messager, C.: Greenhouse gases regional fluxes estimated from atmospheric measurements, Ph. D. thesis, Université Paris 7 – Denis Diderot, available at: http://tel.archives-ouvertes.fr/tel-00164720 (last access: January 2013), 2007.

Miller, J. B., Lehman, S. J., Montzka, S. A., Sweeney, C., Miller, B. R., Karion, A., Wolak, C., Dlugokencky, J., Southon, J., Turnbull, J. C., and Tans, P. P.: Linking emissions of fossil fuel CO_2 and other anthropogenic trace gases using atmospheric $^{14}CO_2$, J. Geophys. Res., 117, D08302, doi:10.1029/2011JD017048, 2012.

Neubert, R. E. M., Spijkervet, L. L., Schut, J. K., Been, H. A., and Meijer, H. A. J.: A computer-controlled continuous air drying and flask sampling system, J. Atmos. Ocean. Tech., 21, 651–659, 2004.

Newman, S., Xu, X., Affek, H. P., Stolper, E., and Epstein, S.: Changes in mixing ratio and isotopic composition of CO_2 in urban air from the Los Angeles basin, California, between 1972 and 2003, J. Geophys. Res.-Atmos. (1984–2012), 113, doi:10.1029/2008JD009999, 2008.

Olivier, J. G. J. and Berdowsky, J. J. M.: Global emissions sources and sinks, in: The Climate System, edited by: Berdowski, J., Guicherit, R., and Heij, B. J., 33–78. A.A. Balkema Publishers/Swets & Zeitlinger Publishers, Lisse, The Netherlands, ISBN 90 5809 255 0, 2001.

Olivier, J. G. J., Berdowski, J. J. M., Peters, J., Bakker, J., Visschedijk, A. J. H., and Bloos, J. P. J.: Applications of EDGAR. Including a description of EDGAR 3.0: reference database with trend data for 1970–1995, RIVM, Bilthoven. RIVM report no. 773301 001/NOP report no. 410200 051, 2001.

Pataki, D. E., Ehleringer, J. R., Flanagan, L. B., Yakir, D., Bowling, D. R., Still, C. J., Buchmann, N., Kaplan, J. O., and Berry, J. A.: The application and interpretation of Keeling plots in terrestrial carbon cycle research, Global Biogeochem. Cy., 17, 1022, doi:10.1029/2001GB001850, 2003.

Pataki, D. E., Bowling, D. R., Ehleringer, J. R., and Zobitz, J. M.: High resolution atmospheric monitoring of urban carbon dioxide sources, Geophys. Res. Lett., 33, doi:10.1029/2005GL024822, 2006.

Pépin, L., Schmidt, M., Ramonet, M., Worhty, D. E. J., and Ciais, P.: A new gas chromatographic experiment to analyse greehouse gases in flask samples and ambient air in the region of Saclay, Tech. rep., IPSL, available at: www.lmd.polytechnique.fr/nai/nai_27.pdf, 2001.

Peylin, P., Rayner, P. J., Bousquet, P., Carouge, C., Hourdin, F., Heinrich, P., Ciais, P., and AEROCARB contributors: Daily CO_2 flux estimates over Europe from continuous atmospheric measurements: 1, inverse methodology, Atmos. Chem. Phys., 5, 3173–3186, doi:10.5194/acp-5-3173-2005, 2005.

Peylin, P., Houweling, S., Krol, M. C., Karstens, U., Rödenbeck, C., Geels, C., Vermeulen, A., Badawy, B., Aulagnier, C., Pregger, T., Delage, F., Pieterse, G., Ciais, P., and Heimann, M.: Importance of fossil fuel emission uncertainties over Europe for CO_2 modeling: model intercomparison, Atmos. Chem. Phys., 11, 6607–6622, doi:10.5194/acp-11-6607-2011, 2011.

Rayner, P. and Law, R.: The interannual variability of the global carbon cycle, Tellus B, 51, 210–212, 1999.

Roberts, J. M., Fehsenfeld, F. C., Liu, S. C., Bollinger, M. J., Hahn, C., Albritton, D. L., and Sievers, R. E.: Measurements of aromatic hydrocarbon ratios and NO_x concentrations in the rural troposphere: Observation of air mass photochemical aging and NO_x removal, Atmos. Environ. (1967), 18, 2421–2432, 1984.

Rödenbeck, C.: Estimating CO_2 sources and sinks from atmospheric mixing ratio measurements using a global inversion of atmospheric transport, Tech. rep., MPI BGC, 2005.

Rödenbeck, C., Houweling, S., Gloor, M., and Heimann, M.: CO_2 flux history 1982–2001 inferred from atmospheric data using a global inversion of atmospheric transport, Atmos. Chem. Phys., 3, 1919–1964, doi:10.5194/acp-3-1919-2003, 2003.

Royer, P., Chazette, P., Sartelet, K., Zhang, Q. J., Beekmann, M., and Raut, J.-C.: Comparison of lidar-derived PM_{10} with regional modeling and ground-based observations in the frame of MEGAPOLI experiment, Atmos. Chem. Phys., 11, 10705–10726, doi:10.5194/acp-11-10705-2011, 2011.

Schmidt, M., Ramonet, M., Wastine, B., Delmotte, M., Galdemard, P., Kazan, V., Messager, C., Royer, A., Valant, C., Xueref, I., and Ciais, P.: RAMCES: The French Network of Atmospheric Greenhouse Gas Monitoring, in WMO/GAW report 168, in: The 13th WMO/IAEA Meeting of Experts on Carbon Dioxide Concentration and Related Tracers Measurement Techniques, 1359, 2005.

Stohl, A., Burkhart, J. F., Eckhardt, S., Hirdman, D., and Sodemann, H.: An integrated internet-based system for analyzing the influence of emission sources and atmospheric transport on measured concentrations of trace gases and aerosols, Tech. rep., NILU, Norway, 2007.

Stuiver, M. and Polach, H. A.: Reporting of ^{14}C data, Radiocarbon, 19, 355–363, 1977.

Tans, P. P.: $^{13}C/^{12}C$ of industrial CO_2, Carbon Cycle Modelling, SCOPE, 16, 127–129, 1981.

Thompson, R. L., Gerbig, C., and Rödenbeck, C.: A Bayesian inversion estimate of N_2O emissions for western and central Europe and the assessment of aggregation errors, Atmos. Chem. Phys., 11, 3443–3458, doi:10.5194/acp-11-3443-2011, 2011.

Turnbull, J. C., Miller, J. B., Lehman, S. J., Tans, P. P., Sparks, R. J., and Southon, J.: Comparison of $^{14}CO_2$, CO, and SF_6 as tracers for recently added fossil fuel CO_2 in the atmosphere and implications for biological CO_2 exchange, Geophys. Res. Lett., 33, L01817, doi:10.1029/2005GL024213, 2006.

Turnbull, J. C., Lehman, S. J., Miller, J. B., Sparks, R. J., Southon, J. R., and Tans, P. P.: A new high precision $^{14}CO_2$ time series for North American continental air, J. Geophys. Res, 112, D11310, doi:10.1029/2006JD008184, 2007.

Turnbull, J. C., Karion, A., Fischer, M. L., Faloona, I., Guilderson, T., Lehman, S. J., Miller, B. R., Miller, J. B., Montzka, S., Sherwood, T., Saripalli, S., Sweeney, C., and Tans, P. P.: Assessment of fossil fuel carbon dioxide and other anthropogenic trace gas emissions from airborne measurements over Sacramento, California in spring 2009, Atmos. Chem. Phys., 11, 705–721, doi:10.5194/acp-11-705-2011, 2011.

van der Laan, S., Neubert, R. E. M., and Meijer, H. A. J.: Methane and nitrous oxide emissions in The Netherlands: ambient measurements support the national inventories, Atmos. Chem. Phys., 9, 9369–9379, doi:10.5194/acp-9-9369-2009, 2009.

Vogel, F. R., Hammer, S., Steinhof, A., Kromer, B., and Levin, I.: Implication of weekly and diurnal ^{14}C calibration on hourly estimates of CO-based fossil fuel CO_2 at a moderately polluted site in southwestern Germany, Tellus B, 62, 512–520, 2010.

Warneke, C., McKeen, S., De Gouw, J., Goldan, P., Kuster, W., Holloway, J., Williams, E., Lerner, B., Parrish, D., Trainer, M., et al.: Determination of urban volatile organic compound emission ratios and comparison with an emissions database, J. Geophys. Res.-Atmos. (1984–2012), 112, doi:10.1029/2006JD007930, 2007.

Wastine, B., Kaiser, C., Vuillelin, C., Lavric, J. V., Schmidt, M., and Ramonet, M.: Evaluation of the EnviroSense 3000i analysers for continuous CO_2/CH_4 measurements by CRDS , Tech. rep., LSCE-CEA-CNRS-IPSL, 2009.

Werner, R. A., Rothe, M., and Brand, W. A.: Extraction of CO_2 from air samples for isotopic analysis and limits to ultra high precision $\delta^{18}O$ determination in CO_2 gas, Rapid Commun. Mass Sp., 15, 2152–2167, 2001.

Widory, D. and Javoy, M.: The carbon isotope composition of atmospheric CO_2 in Paris, Earth Planet. Sci. Lett., 215, 289–298, 2003.

WMO-GAW (Ed.): 13th WMO/IAEA Meeting of Experts on Carbon Dioxide, Other Greenhouse Gases, and Related Tracer Measurement Techniques, vol. 168, Global Atmosphere Watch, Boulder, Colorado, USA, 2005.

WMO-GAW (Ed.): 15th WMO/IAEA Meeting of Experts on Carbon Dioxide, Other Greenhouse Gases, and Related Tracer Measurement Techniques, vol. 194, Global Atmosphere Watch, Jena, Germany, 2009.

Yver, C., Schmidt, M., Bousquet, P., Zahorowski, W., and Ramonet, M.: Estimation of the molecular hydrogen soil uptake and traffic emissions at a suburban site near Paris through hydrogen, carbon monoxide, and radon-222 semicontinuous measurements, J. Geophys. Res., 114, D18304, doi:10.1029/2009JD012122, 2009.

Yver, C., Schmidt, M., Bousquet, P., and Ramonet, M.: Measurements of molecular hydrogen and carbon monoxide on the Trainou tall tower, Tellus B, 2010.

Zondervan, A. and Meijer, H. A. J.: Isotopic characterisation of CO_2 sources during regional pollution events using isotopic and radiocarbon analysis, Tellus B, 48, 601–612, 1996.